

1 Mixed Compounds of $Cd_{1-x}Mg_xO$ ($0 \leq x \leq 1$ and their Optoelectronic Properties

2
3 Adewumi I. Popoola^{1*}, Agboola B. Samuel²

4
5 ^{1,2}Department of Physics,
6 Federal University of Technology,
7 P. M. B. 704 Akure, NIGERIA.

8
9
10
11 **ABSTRACT**

The engineering of bandgap in materials is desired to develop new optoelectronic and photonic devices. The structure, electronic and optical properties of MgO (an insulator) mixed with CdO (a semiconductor) in the stoichiometry $Cd_{1-x}Mg_xO$ ($0 \leq x \leq 1$) are calculated using the ab initio density functional theory. The bond character changes from partial covalent to a more stronger covalent bond as Cd concentration increases in MgO. The dominant covalent bond, coupled with high bulk modulus values predicts that the mixed compounds are hard materials and that Cd and Mg compliments each other to increase the hardness. All the mixed compounds are indirect bandgap materials. The dielectric function and the refractive index shifts to lower energy domain as Cd concentration increases, indicating that the optoelectronic property of the compounds is Cd dependent. The evaluated optoelectronic property predicts the material to be effective for applications in the visible and UV regions of the energy spectrum.

12
13 *Keywords: Bandgap, covalent bond, dielectric function, refractive index*

14 **1. INTRODUCTION**

15 Due to their distinctive physical properties and wide application areas, considerable attention
16 have been devoted to the understanding of the oxides of group II-VI elements. A member of
17 this group is magnesium oxide (MgO). Stoichiometrically, MgO is an insulator with a cubic
18 sodium chloride (NaCl) rock-salt structure. Its experimental band gap (E_g) has been quoted
19 to range between 4.6 and 7.8 eV. It has melting temperature [1-4]. Another member of this
20 group is cadmium oxide (CdO). It is a semiconductor with a band gap of 0.85 eV at room
21 temperature. Its normal structure is also the cubic sodium chloride (NaCl) rock-salt (see Fig.
22 1(a)), which can under pressure, undergo a first-order structural phase transition from the
23 NaCl to the cesium-chloride (CsCl) structure [5]. Because CdO is optically transparent and
24 electrically conductive, it is widely used as window for solar cells. With careful manipulation
25 of CdO bandgap, it can serve as an effective photocatalyst for the degradation of organic
26 pollutants [6]. On the other hand, MgO have shown prospect for high-temperature
27 superconductor and ferroelectric material production [7, 8]. Thin layers of MgO are used as
28 dielectrics both to improve discharge characteristics and lifetime in plasma screens [9]. The
29 cadmium in CdO is toxic. The production of nano-composite to overcome the problem, have
30 been discussed [10]. MgO is non-toxic and with appropriate doping, it can serve as material
31 for radiation dosimetry [11]. It is a material of choice as antireflection layer in solar cells and
32 as the insulating material for the gates of Field Effect Transistors.

33
34 In materials science, it is a common knowledge that the magnitude/size of E_g , will affect the
35 optoelectronic as well as the photonic properties of the material. With addition of element(s)
36 into a lattice (through doping or full/partial substitution), a change in E_g can be achieved. The

*Email address: aipopoola@futa.edu.ng

37 adjustment of E_g in insulating/semiconducting compounds and the impact of such
 38 adjustment on the electronic, optoelectronic and the photonic properties of the material must
 39 be understood in order to design new functional devices. In the present theoretical work, the
 40 bandgap of the rock salt MgO (an insulator) is varied systematically by alloying with that of
 41 CdO (a semi-metal). In order to understand the optoelectronic nature of these alloys, their
 42 structural, electronic and optical properties are investigated.

43

44 2. CALCULATION METHODS

45 All calculation is performed using the plane-wave pseudo-potential Density Functional
 46 Theory (DFT), of which its one particle Schrödinger equation is written as [12, 13]:

47

$$48 \left[\frac{-1}{2} \nabla^2 + V_c(r) + \mu_{xc}(r) \right] \psi_i(r) = \varepsilon \psi_i(r), \quad (1)$$

49

50 where $\frac{-1}{2} \nabla^2$ is the kinetic energy, $V_c(r)$ is the Coulomb energy and $\mu_{xc}(r)$ is the exchange-
 51 correlation. The solutions to (1) are one-particle wave-functions related to the total electron
 52 density as:

53

$$54 \rho(r) = \sum_i n_i \psi_i(r) \quad (2)$$

55

56 where n_i is the i^{th} state occupation number. The unknown wave-function $\psi_i(r)$, is usually
 57 expanded in terms of known basis functions $\varphi_j(r)$ with unknown linear expansion coefficients
 58 c_{ij} as:

59

$$60 \psi_i(r) = \sum_j c_{ij} \varphi_j(r), \quad (3)$$

61

62 The unknown coefficients c_{ij} are obtained by applying variational procedure to solve a matrix
 63 of the form:

64

$$65 (H - \varepsilon S)c = 0, \quad (4)$$

66

67

68

69

70

71

72

73

74

75

76

77

78

79

80

81

82

83

84

85

86

87

88

89

90

91

92

93

94

95

96

97

$$E(V) = E_0 + \frac{B_0 V}{B'_0} \left(\frac{\left(\frac{V_0}{V} \right)^{B'_0}}{B'_0 - 1} + 1 \right) - \frac{B_0 V_0}{B'_0 - 1}, \quad (7)$$

*Email address: aipopoola@futa.edu.ng

84 where E_0 is the total energy of the supercell, V is the unit volume, B_0 is the bulk modulus at
 85 zero pressure and B'_0 is the derivative of bulk modulus with pressure.

86
 87 There is a relationship between the optical properties of a material and its dielectric function
 88 (ϵ). The two parts to the dielectric function; the real and the imaginary parts are given as:

89
 90
$$\epsilon(\omega) = \epsilon_1(\omega) + i\epsilon_2(\omega) \quad (8)$$

91
 92 For the $Cd_{1-x}Mg_xO$ ($0 \leq x \leq 1$) mixed compounds, the imaginary and the real parts can be
 93 calculated using [19, 20]:

94
$$\epsilon_2(\omega) = \frac{8}{2\pi\omega^2} \sum_{nn'} \int |p_{nn'}(k)|^2 \frac{dSk}{V\omega_{nn'}(k)} \quad (9)$$

95
 96
$$\epsilon_1(\omega) = 1 + \frac{2}{\pi} p \int_0^\infty \frac{\omega' \epsilon_2(\omega')}{\omega'^2 - \omega'^2} d\omega' \quad (10)$$

97
 98 The refractive index can be calculated in terms of the real and the imaginary parts of the
 99 dielectric function by the following relation:

100

$$\frac{\omega}{\omega} = \frac{2 + \epsilon_2}{\epsilon_1} \quad (11)$$

102
$$n(\omega) = \frac{1}{\sqrt{2}}$$

103 and the absorption coefficient can be calculated by:

104
 105
$$\alpha(\omega) = \frac{\omega \epsilon_2(\omega)}{c} \quad (12)$$

106
 107 Since all the functions in (8) – (11) depend on the electronic band structure, they can thus be
 108 easily evaluated from DFT calculations.

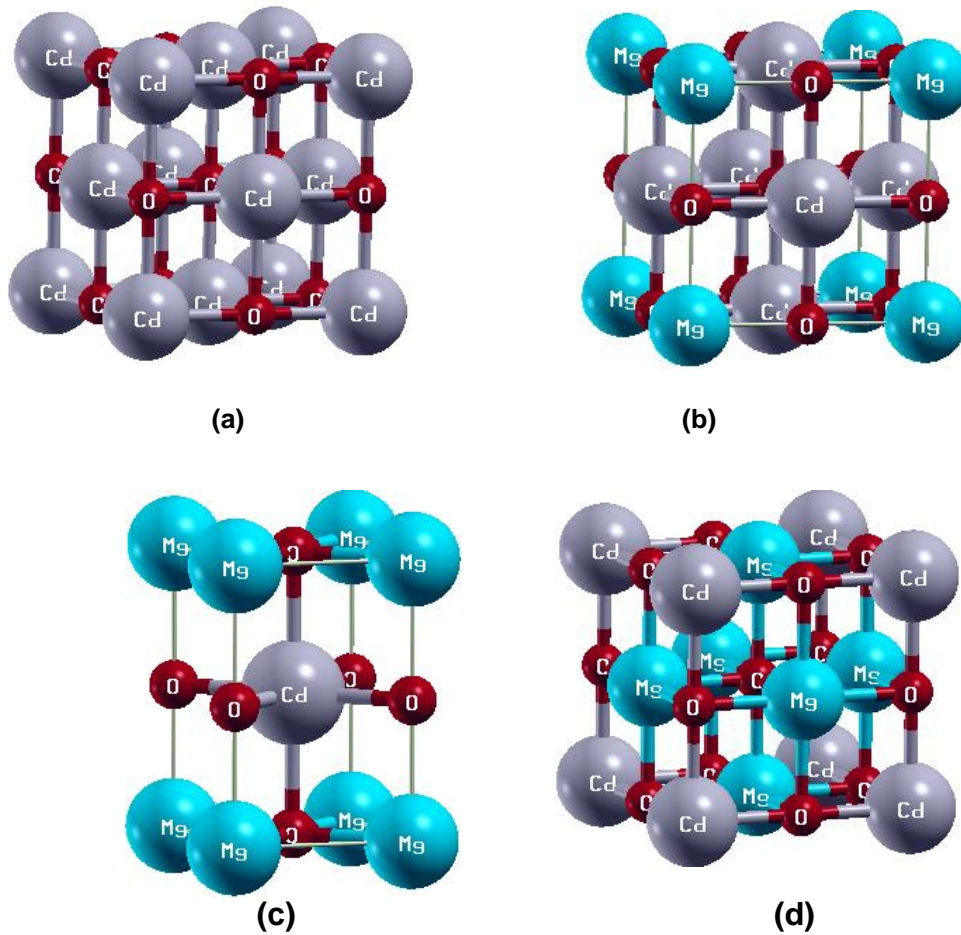
109
 110 **3. RESULTS AND DISCUSSION**

111 The composition of Cd at a step of 0.25 in MgO resulted significantly into different crystal
 112 structure as shown in Fig. 1 (b) – (d). The atomic mass of Cd (112.41 g) is quite large,
 113 compared to that of Mg (24.31 g). This is suspected to have impacted on the atomic volumes
 114 and therefore the change in the crystal structure of $Cd_{1-x}Mg_xO$ ($0 \leq x \leq 1$, as the
 115 concentration of Mg increases from 0 to 100%. Due to the volume change, the space group
 116 of the structure obtained also changed from Fm-3m to Pm-3m at ratio 3:1 (see Fig. 1b) of Cd
 117 to Mg ($Cd_{0.75}Mg_{0.25}O$), A similar space group is obtained at ratio 1:3 (see Fig. 1d) of Cd
 118 to Mg ($Cd_{0.25}Mg_{0.75}O$). At a ratio of 1:1 of Cd to Mg ($Cd_{0.50}Mg_{0.50}O$), the structure changes from
 119 cubic to tetragonal as shown in Fig. 1(c).

120
 121 The calculated lattice constant (LP), bulk modulus (B_0) and the band-gaps (E_g) are
 122 presented in Table 1. The experimental data on the binary compounds (MgO and CdO)

*Email address: aipool@futa.edu.ng

123 deviates from theoretical results. This is not surprising because theoretical bandgap data
 124 are usually underestimated by DFT calculation. The trend seen in LP as Cd substitutes Mg is
 125 expected, as the atomic radius of Cd (144 pm) is slightly higher than for Mg (141 pm).
 126 However, despite the systematic variation in the LP, a huge difference can be seen in the
 127 bulk modulus as Cd supplants Mg in MgO. When 25% Mg is substituted with Cd in MgO
 128 ($Cd_{0.25}Mg_{0.75}O$), B_0 rose from 149.3 GPa to 614.2 GPa (an increment that is well above
 129 300%). On the Vickers scale, B_0 relates directly with materials hardness [21]. Thus, it can be
 130 concluded that Cd in MgO is an excellent hardener, where the level of hardness depends
 131 majorly on Cd content.



145
146
147
148
149
150
151
152
153
154
155
156
157
158
159
160
161
162
163 **Fig. 1. Crystal structure of (a) CdO, (b) $Cd_{0.75}Mg_{0.25}O$ (c) $Cd_{0.5}Mg_{0.5}O$ and (d)**
 164 **$Cd_{0.25}Mg_{0.75}O$**

165
166 The band structure for CdO and MgO are shown in figures 2 and 3. The projected density of
 167 states is also presented alongside in order to understand bonding and the origin of these
 168 bands. It is evident from Fig. 3 that MgO is an insulator. Its bands are scanty both in the
 169 conduction and the valence band. Also, a wide bandgap is seen in its band diagram. On the
 170 other hand, a narrow bandgap coupled with denser bands are seen in the band diagram of

*Email address: aipool@futa.edu.ng

171 CdO (see figure 2). Both MgO and CdO are direct bandgap materials. The conduction and
 172 valence bands of CdO are influenced by Cd-2s, Cd-3p and O-2p orbitals. In MgO, the
 173 activities at the valence band are influenced solely by O-2p while it is influenced at the
 174 conduction band by Mg-3s and O-2p orbitals. Going by the Pauling Scale, the electro-
 175 negativity difference between Cd (1.69), Mg (1.31) and O (3.04) indicates that covalent bond
 176 dominates in CdO than in MgO. When this information is combined with their respective high
 177 B_0 values, CdO and MgO are hard and brittle materials.

178

179 Table 1: Calculated lattice constants (LP), bulk modulus (B_0) and bandgap (E_g) for mixed
 180 compounds of $Cd_{1-x}Mg_xO$ ($0 \leq x \leq 1$). Experimental data are in bracket and are from [22].

181

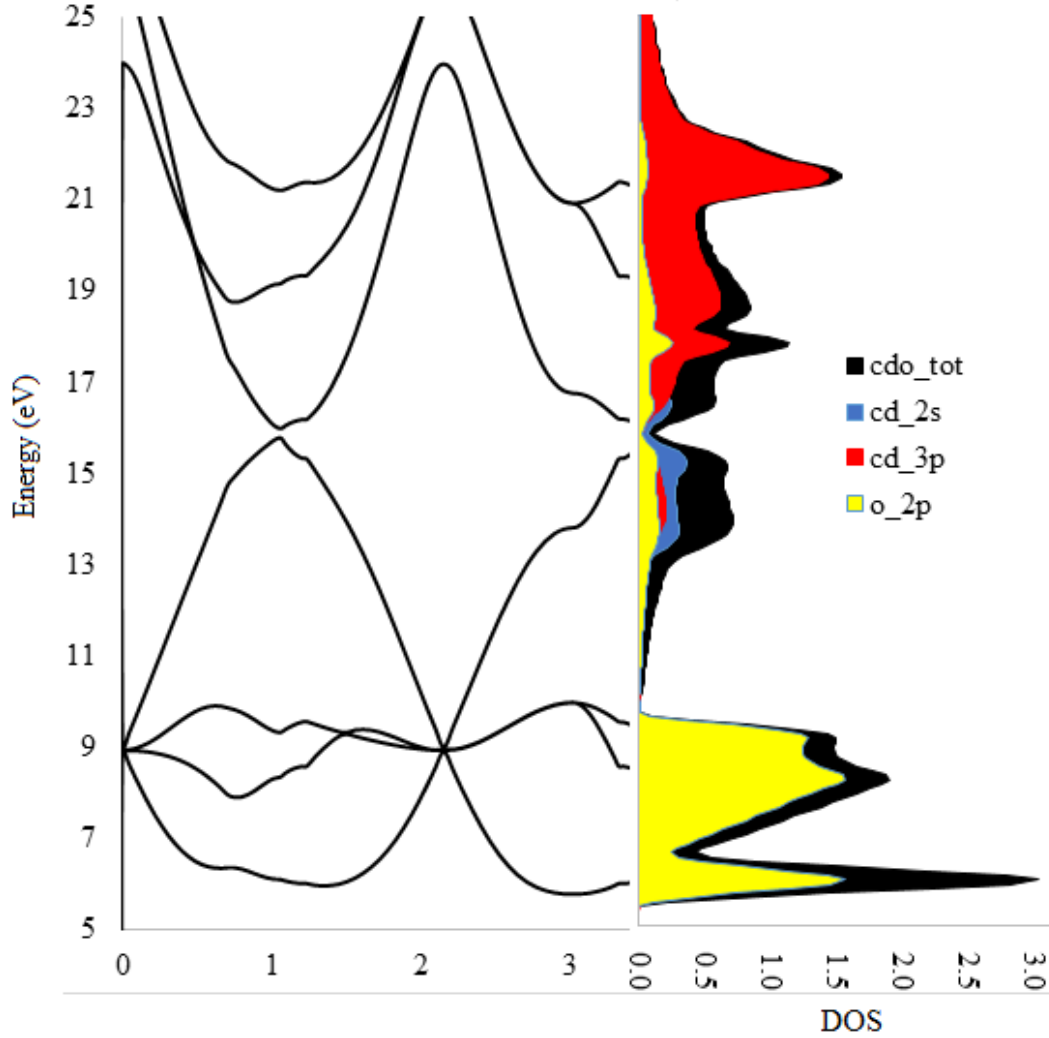
Alloy	LP (Å)	B_0 (GPa)	E_g (eV)
MgO	4.249	149.3	3.216 [7.00]
$Cd_{0.25}Mg_{0.75}O$	4.391	614.2	1.185
$Cd_{0.5}Mg_{0.5}O$	4.431; 4.775	600.0	0.684
$Cd_{0.75}Mg_{0.25}O$	4.476	689.3	0.013
CdO	5.372	29.30	0.303 [0.85]

188

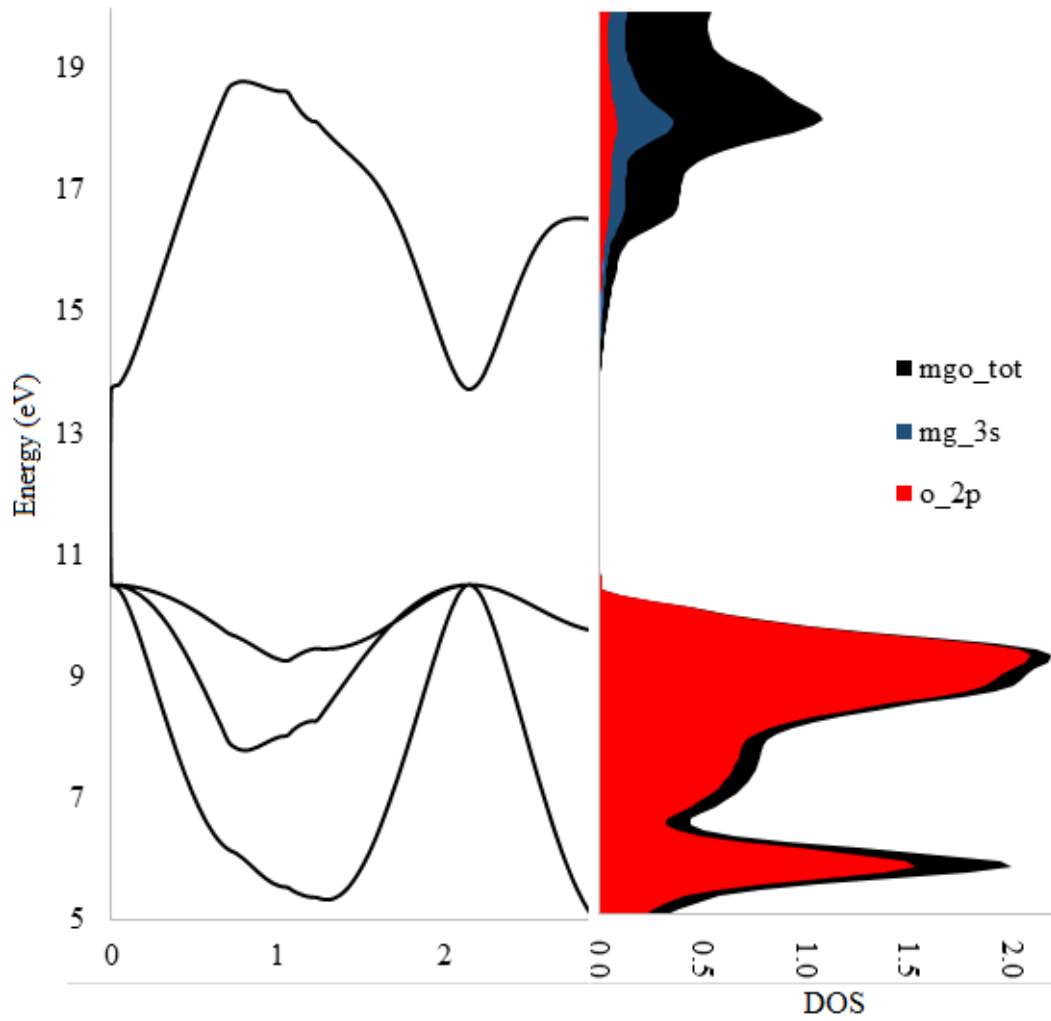
189 The band diagram for the compound in which the ratio of Mg to Cd is 1:3 ($Cd_{0.75}Mg_{0.25}O$) is
 190 shown in Fig. 4. The band diagram for the compound in which the ratio of Mg to Cd is 3:1
 191 ($Cd_{0.25}Mg_{0.75}O$) is shown in Fig. 5, while that for which Mg to Cd is in ratio 1:1 is shown in
 192 Figure 6. It can be predicted from Figures 4 - 6 that $Cd_{1-x}Mg_xO$ ($0.25 \leq x \leq 0.75$) mixed
 193 compounds are indirect bandgap materials. The nature of the bandgap is not affected even
 194 as Cd substitutes Mg. Rather, the bandgap decreases from 3.216 eV (for MgO) down to
 195 0.134 eV (for $Cd_{0.75}Mg_{0.25}O$). In Figure 4, O-2p orbital is solely responsible for bonding and
 196 the band character at the valence and conduction bands. It is therefore interesting to see
 197 that while Cd-2s, Cd-3p and O-2p are responsible for orbital hybridization in CdO, the story
 198 is quite different when one Cd is replaced with Mg (giving $Cd_{0.75}Mg_{0.25}O$). The interchange of
 199 state seen is due to a change in the nature of the bonding. The electronegativity of Cd > Mg,
 200 hence, a decrease in the dominant nature of covalent bonding is expected with increase in
 201 Mg content. In this light, O-2p dominates at the valence band, while Cd-3p and O-2p are
 202 responsible for the band character at the conduction band in $Cd_{0.25}Mg_{0.75}O$ (Fig. 5). Likewise,

*Email address: aipopoola@futa.edu.ng

203 at 50% composition of Mg to Cd in $Cd_{0.5}Mg_{0.5}O$, O-2p dominates at the valence band, while
204 Cd-3p and O-2p are responsible for the band character at the conduction band. In
205 comparison with MgO, partial covalent bonding is predominant in $Cd_{1-x}Mg_xO$ ($0.25 \leq x \leq$
206 0.75 , hence the reason for their respective high B_0 values.

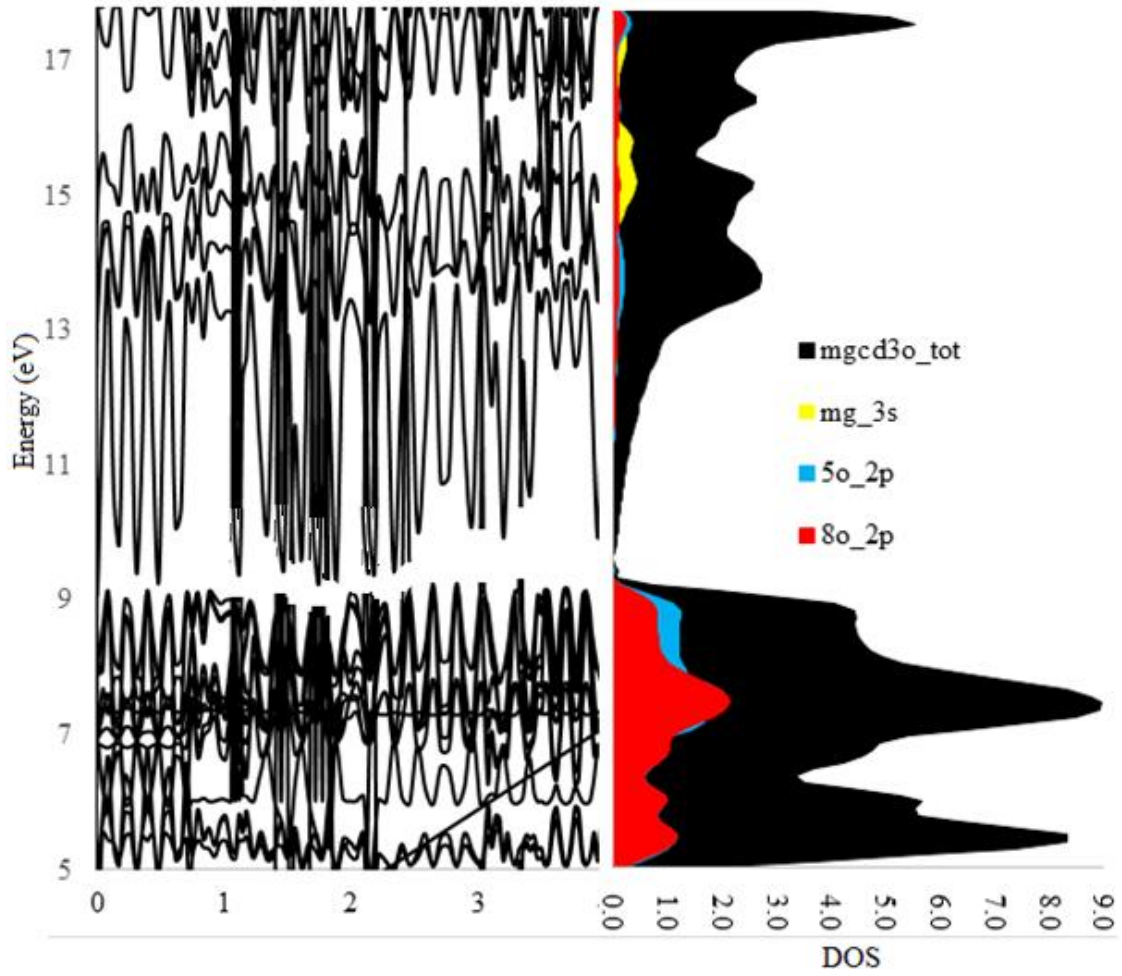


207
208 **Fig. 2. Calculated band structure for CdO**



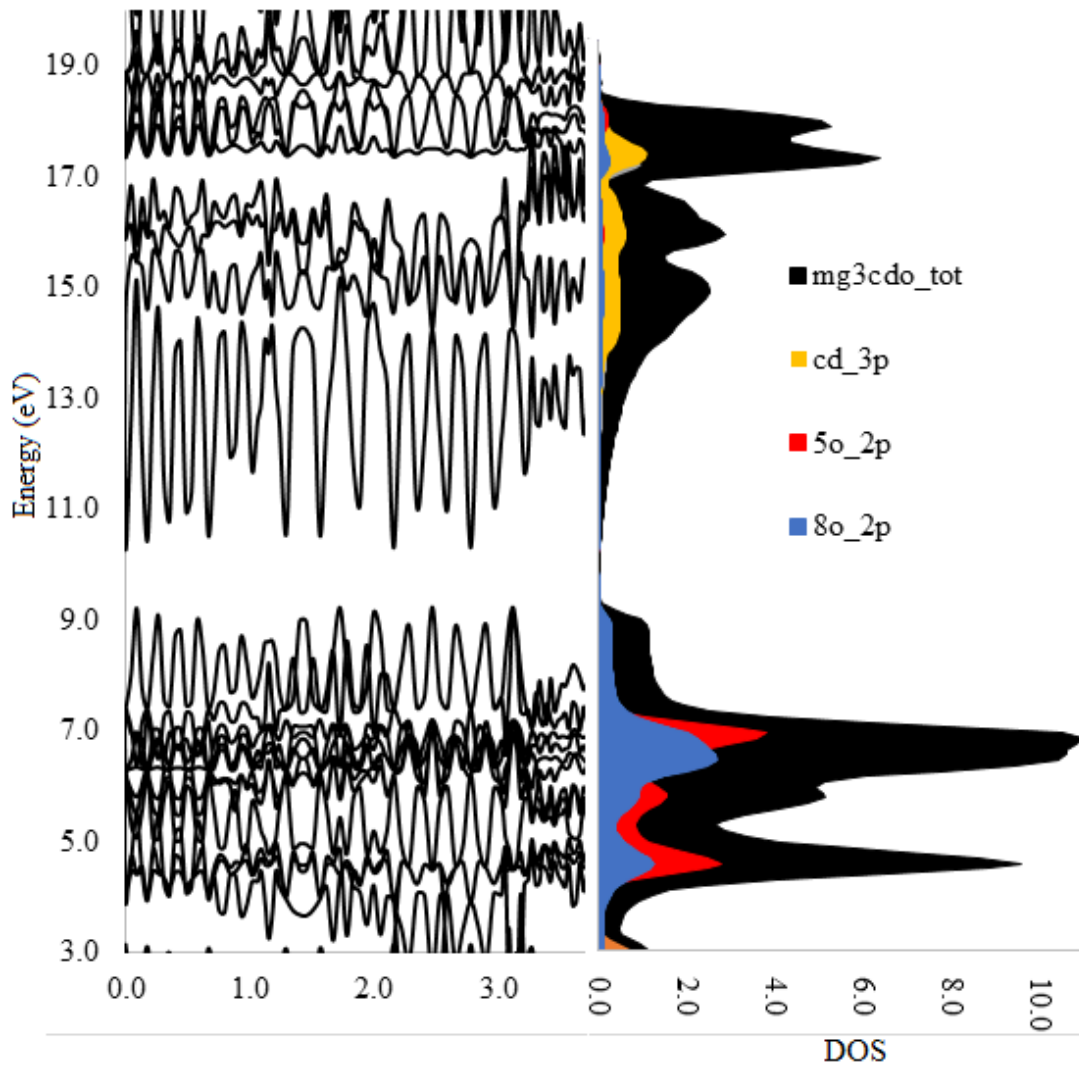
209
 210
 211
 212
 213

Fig. 3. Calculated band structure for MgO



214
215
216

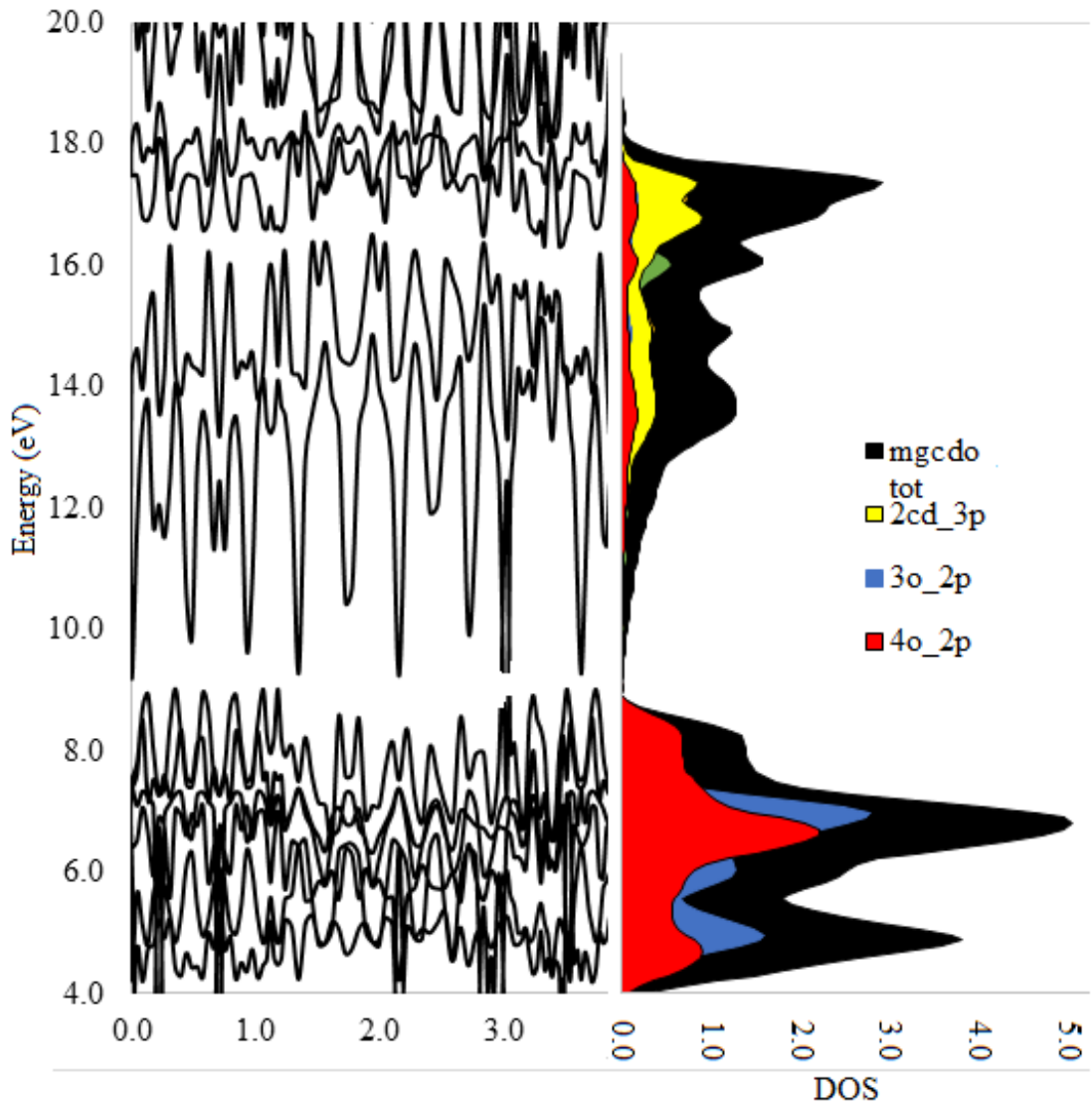
Fig. 4. Calculated band structure for $\text{Cd}_{0.75}\text{Mg}_{0.25}\text{O}$



217
 218
 219
 220
 221
 222
 223
 224
 225
 226
 227
 228
 229
 230
 231
 232
 233
 234
 235

Fig. 5. Calculated band structure for $Cd_{0.25}Mg_{0.75}O$

*Email address: aipopoola@futa.edu.ng



236
 237
 238
 239
 240
 241
 242
 243
 244
 245
 246
 247
 248
 249
 250
 251
 252

Fig. 6. Calculated band structure for CdMgO

253 Materials with bandgap (E_g) are required for optoelectronic applications. Available evidence
254 [23, 24] has shown that materials with $E_g \leq 3.1$ eV work well for devices working within the
255 visible region of energy spectrum while those with $E_g > 3.1$ eV are good for devices working
256 within the UV region. The mixture of MgO (an insulator) with CdO (a semiconductor) in
257 $Cd_{1-x}Mg_xO$ ($0 \leq x \leq 1$ stoichiometry should provide promising devices whose bandgap
258 would vary between 0.85 and 7.00 eV. The calculated E_g results in Table 1, especially for
259 the binary compounds (MgO and CdO) are lower compared to experimental E_g . This is to be
260 expected because DFT usually underestimate E_g . Despite the underestimation, it is
261 predicted that $Cd_{1-x}Mg_xO$ ($0.25 \leq x \leq 0.75$ compounds should suite optoelectronic
262 applications both in the visible and ultraviolet (UV) regions. To understand the prominent
263 variations in the optical absorption behavior of the materials, the calculated dielectric
264 function (the imaginary part) in the 0–25 eV energy range is shown in Fig. 7. It is evident
265 from this figure that the absorption of MgO is somewhat between 4.8 and 18 eV with its
266 critical point at about 11.2 eV. As the concentration of Cd increases, the width and critical
267 points of the absorption region shift toward lower energy, except for $Cd_{0.5}Mg_{0.5}O$ where the
268 critical point is maintained at almost 11.2 eV and this may be attributed to the structural
269 change (cubic to tetragonal) that occurred at that composition.

270

271 A plot of $n(\omega)$ for $Cd_{1-x}Mg_xO$ ($0 \leq x \leq 1$ is shown in Fig. 8. There are two things that are
272 obvious here. First, a broad spectrum of $n(\omega)$ over wide energy range is noted. The
273 $n(\omega)$ maxima shift to lower energy region with increase in Cd concentration. Secondly, $n(\omega)$
274 drops below unity at certain energy ranges. Any $n(\omega)$ lesser than unity means that v_g (the
275 group velocity) of the wave packet is larger than c ($v_g = \frac{c}{n}$). In other words, at $n(\omega) < 1$, v_g
276 would shifts to the negative domain and hence, the material becomes superluminal for high
277 energy incident photons [25, 26].

278

279

4. CONCLUSION

280 For the first time, the Density functional calculation method have been performed to
281 investigate the structure and the optoelectronic properties of compounds formed from
282 systematic mixture of MgO and CdO in ratio $Cd_{1-x}Mg_xO$ ($0 \leq x \leq 1$. At equal concentration of
283 Cd to Mg, structure change from cubic to tetragonal is predicted. The bonding nature in the
284 materials significantly varies with Cd resulting in extremely hard materials. All the mixed
285 compounds have indirect bandgaps according to their calculated band structure. It can be
286 concluded that with appropriate experimental procedure, the material can be used in
287 optoelectronic applications working in the visible and UV regions of spectrum.

288

289

Competing interests

290

The authors hereby declare that no competing interest exists.

291

292

Authors' Contributions

293

The first author designed the study, performed the calculations and wrote the first draft of the
294 manuscript. The second author performed the statistical analysis. Both author read and
295 approved the final manuscript.

296

297

298

299

300

301

302

303

304
305
306
307
308
309
310
311
312
313
314
315
316
317
318
319
320
321
322
323
324
325
326
327
328
329
330
331
332
333
334
335
336
337
338
339
340
341
342
343
344
345
346
347
348
349
350
351
352
353
354
355

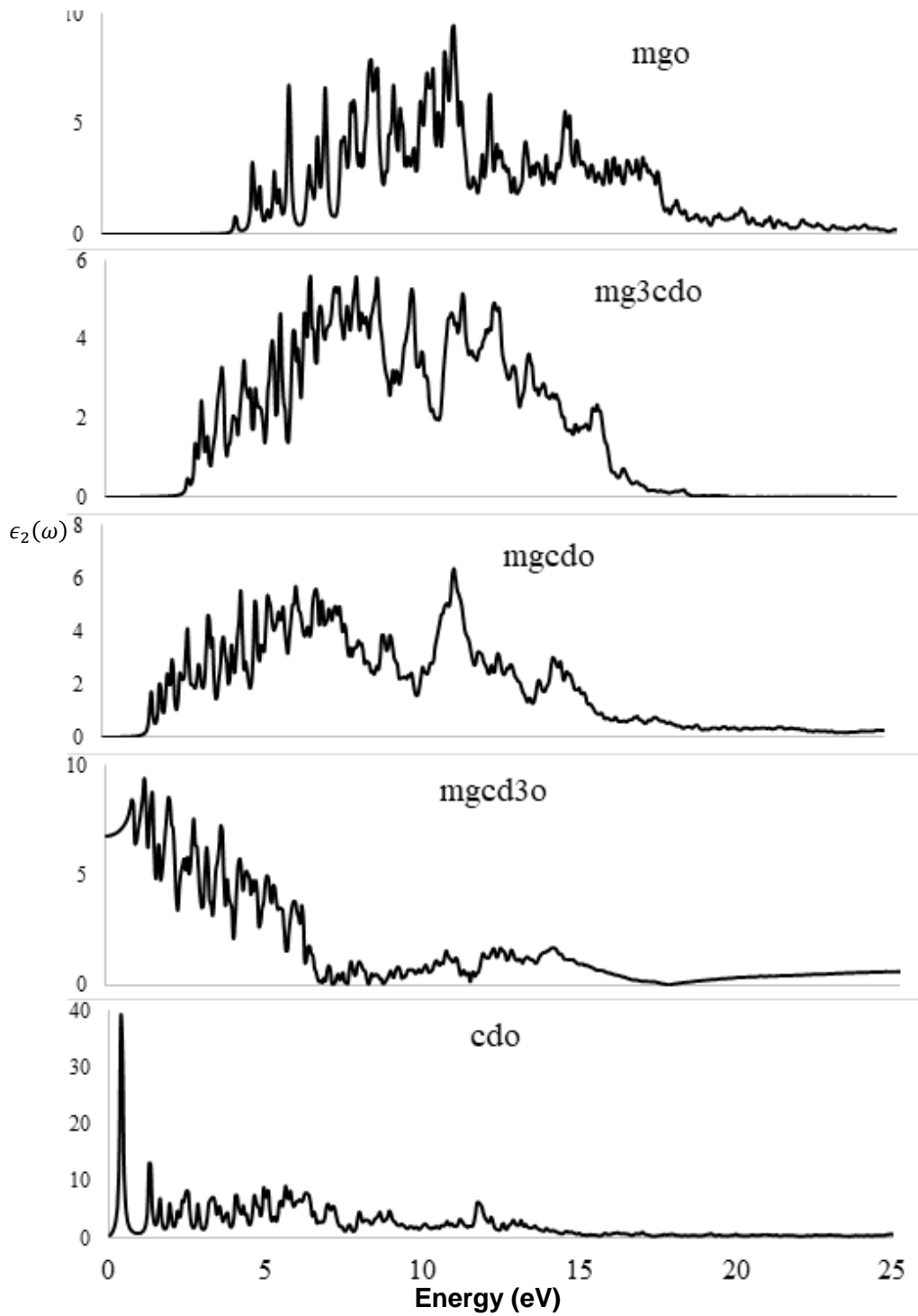


Fig. 7. Frequency dependent imaginary part of dielectric functions of $\text{Cd}_{1-x}\text{Mg}_x\text{O}$ ($0 \leq x \leq 1$)

*Email address: aipopoola@futa.edu.ng

356
357
358
359
360
361
362
363
364
365
366
367
368
369
370
371
372
373
374
375
376
377
378
379
380
381
382
383
384
385
386
387
388
389
390
391
392
393
394
395
396
397
398
399
400
401
402
403
404
405
406
407
408

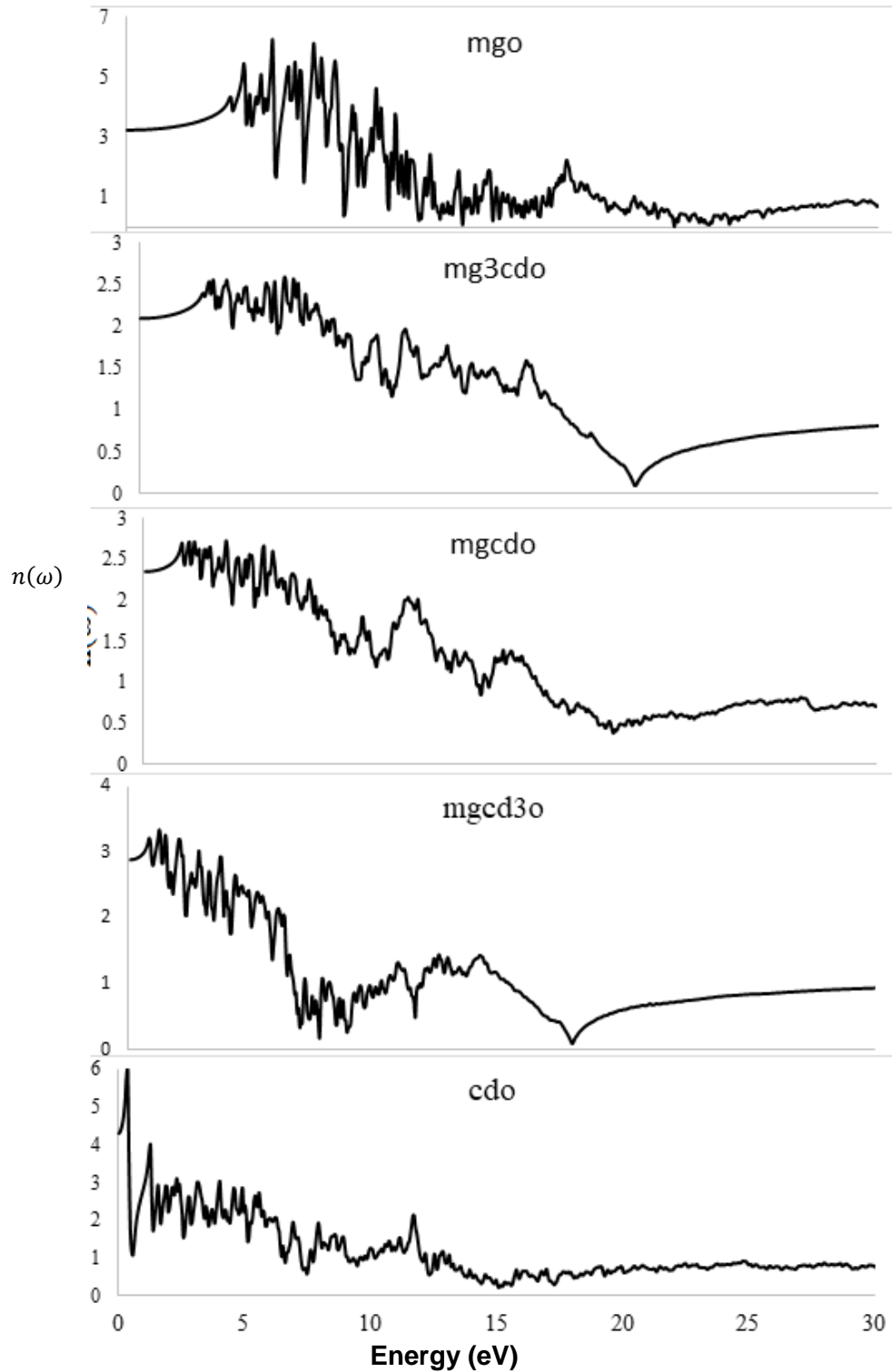


Fig. 8. Frequency dependent refractive indices of $\text{Cd}_{1-x}\text{Mg}_x\text{O}$ ($0 \leq x \leq 1$)
REFERENCES

*Email address: aipopoola@futa.edu.ng

- 409 [1] Harun G, Demet I. Synthesis of MgO thin films grown by SILAR technique. *Ceramics*
410 *International*. 2018; 01:210.
- 411 [2] Lifeng C, Peng B, Wenxiu L. Preparation of a novel magnesium oxide nanofilm of
412 honeycomb-like structure and investigation of its properties. *Chemical Engineering*
413 *Journal*. 2016; 303:588–595.
- 414 [3] Diachenko OV, Opanasuyk AS, Kurbatov DI, Cheong H. Investigation of Optical
415 Properties of Magnesium Oxide Films Obtained by Spray Pyrolysis Technique. 7th
416 International Conference on Advanced optoelectronics and lasers (CAOL) Ukraine,
417 I. I. Mechnikov National University. 2016; 31-33.
- 418 [4] Hadia NMA, Mohamed HAH. Characteristics and optical properties of MgO nanowires
419 synthesized by solvothermal method. *Materials Science in Semiconductor Processing*.
420 2014;03:049.
- 421 [5] Gang Y, Xinyou A, Hongwen L, Yajun F, Weidong W. Electronic and Optical Properties of
422 Rocksalt CdO: A first-Principles Density-Functional Theory Study. *Modeling and*
423 *Numerical Simulation of Material Science*. 2013; 3:16-19.
- 424 [6] Senthil PK, Ganesh MS, Babu S, Karuthapandian S, Chattopadhyay S.
425 CdO nanospheres: Facile synthesis and bandgap modification for the
426 Superior photocatalytic activity. *Materials Letters*. 2015;151:45-48.
- 427 [7] Dyachenko AV, Opanasuyk AS, Kurbatov DI, Kuznetnov, Cheong H. Effect of substrate
428 temperature on substructural and properties of MgO thin films. *Functional Materials*.
429 2015; 22: 1 – 7.
- 430 [8] Wang WB, Yang Y, Yanguas-Gil A, Chang NN, Girolami GS, and Abelson JR. Highly
431 conformal magnesium oxide thin films by low-temperature chemical vapor deposition
432 from $Mg(H_3BNMe_2BH_3)_2$ and water. *Appl. Phys. Lett*. 2013;102:101605.
- 433 [9] Govindhasamy M, Ramasamy J, Rangasamy T, Manavalan RK. PbO/CdO/ZnO
434 and PbS/CdS/ZnS nanocomposites: Studies on optical, electrochemical and
435 thermal properties. *Journal of Luminescence*. 2016;170:78-89.
- 436 [10] Ikeda S, Miura K, Yamamoto H, Mizunuma K, Gan HD, Endo M et al. A perpendicular-
437 anisotropy CoFeB–MgO magnetic tunnel junction. *Nat. Mater*. 2010;9:721.
- 438 [11] Takumi K, Go O, Takayuki Y. Dosimeter properties of MgO transparent
439 ceramic doped with C. *Radiation Measurements*. 2016;92:93-98
- 440 [12] Kohn W and Sham LJ. Self-Consistent Equations Including Exchange and
441 correlation effects. *Physical Reviews A*. 1965;140:1133-1139.
- 442 [13] Hohenberg P and Kohn W. Inhomogeneous Electron Gas. *Physical Reviews B*.
443 1964;136:864-875.
- 444 [14] Giannozzi P, Baroni S, Bonini N, Calandra M, Car R, Cavazzoni C et al. Quantum
445 Espresso: a modular and open-source software project for quantum simulations of
446 materials *Journal of Physics: Condensed Matter*. 2009;21:395502.
- 447 [15] Vanderbilt D. Soft self-consistent pseudopotentials in generalized eigenvalue formalism.
448 *Phys. Rev. B*. 1990;41:7892-7895.
- 449 [16] Perdew, JP, Burke K, and Ernzerhof M. Generalized Gradient Approximation
450 Made Simple. *Physical Review Letters*. 1996;77:3865.
- 451 [17] Monkhorst HJ and Pack JD. Special points for Brillouin-zone integrations.
452 *Physical Reviews B*. 1976;13:5188 – 5192.
- 453 [18] Murnaghan FD. The Compressibility of Media under Extreme Pressures *Proc. Natl.*
454 *Acad. Sci. USA*. 1994; 30(9):244-247.
- 455 [19] Wooten F. *Optical Properties of Solids*, Academic Press, New York, 1972.
- 456 [20] Fox M. *Optical Properties of Solids*, Oxford University Press, 2001.
- 457 [21] Tian Y, Xu B, Zhao Z. Microscopic theory of hardness and design of novel superhard
458 crystals *Int. J. Refract. Met. Hard Mater*. 2012;33:93–106.
- 459 [22] Khan I, Iftikhar Ahmad, Amin B, Murtaza G, Ali Z. Bandgap engineering of $Cd_{1-x}Sr_xO$.
460 *Physica B*. 2011;406:2509 – 2515.

- 461 [23] Gfroerer TH, Priestley LP, Weindruch FE, Wanless MW. Defect-related density of states
462 in low-bandgap $\text{In}_x\text{Ga}_{1-x}\text{As}/\text{InAs}_y\text{P}_{1-y}$ double heterostructures grown on InP substrates.
463 Appl. Phys. Lett. 2002; 80: 4570.
- 464 [24] Benkhedir ML, Aida MS, Stesmans A, Adriaenssens GJ. Experimental study of the
465 density of states in the band gap of a-Se. J. Optoelectron. Adv. Mater. 2005;7 329 - 332.
- 466 [25] Penn DR. Wave-Number-Dependent Dielectric Function of Semiconductors.
467 Phys. Rev. 1962;128: 2093.
- 468 [26] Wang LJ, Kuzmich A, Dogariu A. Gain-Assisted Superluminal Light Propagation
469 Nature, 2000;406:277-283.
470
471